

Steric Quenching of the Switchable Mirror Effect

Troy C. Messina, Casey W. Miller, and John T. Markert

*Department of Physics, 1 University Station - C1600,
University of Texas at Austin, Austin, TX 78712, USA*

(Dated: August 14, 2018)

Scandium was substituted for yttrium to observe the effect of unit cell size on the optical metal-to-insulator (MIT) transition in the $Y_{1-z}Sc_zH_x$ alloy system. The optical transmittance decreases significantly for $z > 0.10$. Simultaneous electrical resistivity measurements confirm the transition from trihydride to dihydride behavior with increasing z . These observations imply a quenching of the MIT when the unit cell volume falls below a critical level that is consistent with the boundary between trihydride and non-trihydride forming rare-earth elements. A combinatoric model reveals this formation boundary corresponds to two or more Sc per unit cell.

PACS numbers: 61.66Dk; 71.30.+h; 78.66.-w; 73.61.-r

Yttrium and lanthanum thin films have been shown to undergo quick and reversible transitions from a metallic-mirror to a transparent-insulator with small changes in hydrogen content^{1,2}. The metal-to-insulator transition (MIT) is dependent on formation of a trihydride phase in rare-earth metals and occurs between the dihydride and trihydride phases³. Structural studies on La, Y, and their alloys suggest the MIT is related to small displacements of octahedral hydrogen, and not mediated by structural phase transitions^{4,5,6,7,8,9,10}. This work reports on the systematic substitution of Sc for Y to sterically control the incorporation of hydrogen into octahedral interstices. Elemental Sc has too small a unit cell for hydrogen to occupy octahedral interstices, and thus cannot form a trihydride, or undergo the metallic-mirror to transparent-insulator transition at STP. Unlike more complex alloys, such as those with Mg and Y^{11,12,13}, Sc and Y have trivalent, closed-shell d^1s^2 electronic configurations. Because these metals are chemically and structurally similar, we argue that a systematic decrease in unit cell volume due to Sc substitution causes $Y_{1-z}Sc_zH_x$ to cross a volume-limited dihydride/trihydride formation boundary, where the decreasing octahedral site radius prevents hydrogen incorporation. We show that the optical gap seen in $YH_{3-\delta}$ is strongly suppressed in $Y_{1-z}Sc_zH_x$ for $z \approx 0.20$ and greater. For such alloys, only dihydride-like transmittance is observed, and resistivity measurements show increasingly metallic behavior in the fully hydrogenated state with increasing z . The proposed formation limit is discussed in terms of a simple combinatoric model.

We deposited 100 nm thick $Y_{1-z}Sc_z$ films capped with a 10 nm layer of palladium (Pd) on room temperature glass substrates using electron-beam evaporation. Base pressures lower than 10^{-8} torr would increase to 10^{-7} torr upon heating the evaporant metals. Impurities in the vacuum presumably getter to the reactive rare earth metal deposited on the chamber walls returning the base pressure to less than 10^{-8} torr after some time. All films were then deposited at 1 Å/s in a vacuum better than 10^{-8} torr. The Pd prevents oxidation and catalyzes hydrogen gas (H_2) dissociation and absorption. Synthe-

sis of the $Y_{1-z}Sc_z$ alloys and films has been discussed previously¹⁴. The compositional dependence of unit cell lattice parameters of as-deposited and stable dihydride films were measured by $\theta - 2\theta$ x-ray diffraction (XRD). The hcp lattice parameters of the as-deposited films for pure Y were $a = 3.69$ Å and $c = 5.82$ Å, and decreased linearly to $a = 3.31$ Å and $c = 5.12$ Å for pure Sc. A similar linear relation was found for the lattice constant of fcc dihydride films, falling from $a = 5.20$ Å for Y to $a = 4.77$ Å for Sc. The a values for YH_2 and ScH_2 are within 1% of literature values for bulk samples. No oxide or hydroxyl impurities were observed in the XRD measurements. The measured 177 Å³ unit cell volume of the first alloy not to exhibit the MIT ($Y_{0.80}Sc_{0.20}$) is approximately the unit cell volume of Lu, the largest (and only trivalent) rare-earth element that does not form a trihydride. Additionally, the H-H separation distance for $z > 0.10$ inferred from measured lattice parameters becomes less than 2.1 Å, which is reportedly the minimum distance for H to occupy octahedral interstitial sites¹⁵.

At STP, the transition from yttrium dihydride to trihydride takes seconds for films less than 500 nm thick. For our studies, the transition was extended to hours using a mass-flow-controlled mixture of ultra-high purity H_2 diluted with Ar. The flow was directed through a modified reflection grating optical transmission spectrometer ($340 \leq \lambda \leq 960$ nm). A background intensity spectrum, $I_0(\lambda)$, was measured prior to each hydrogen loading, and the transmittance calculated as $T(\lambda) = I_T(\lambda)/I_0(\lambda)$, where $I_T(\lambda)$ is the spectrum measured during hydrogen loading. Four probe electrical resistivity measurements were made simultaneously with the optical spectra during loading using a 1 mm \times 10 mm section of the film outside of the spectrometer beam. The resistivity of the rare-earth layer was approximated assuming the bilayer films act as parallel resistors. The resistivity of Pd was measured independently to be 27–29 $\mu\Omega$ -cm for all hydrogen concentrations. The resistivities of pure Y and Sc were 73 $\mu\Omega$ -cm, and 91 $\mu\Omega$ -cm, respectively.

Optical transmittance measurements for $z \leq 0.10$ show dramatic optical switching properties commensu-

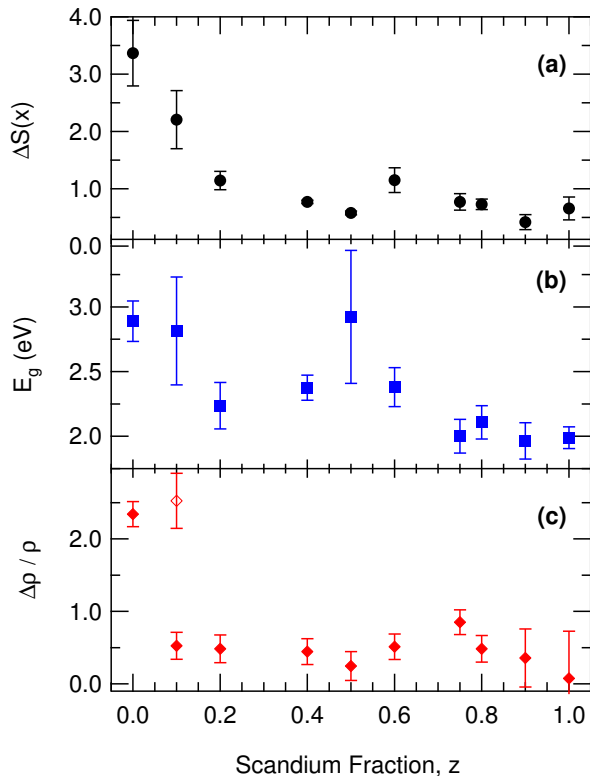


FIG. 1: (Color online) Scandium fraction dependence in $Y_{1-z}Sc_zH_x$ of (a) spectral density transmittance change, (b) best fit optical gap, and (c) relative resistivity change. The symbol, \diamond , is the relative resistivity change between as-deposited and fully hydrogenated $Y_{0.9}Sc_{0.1}H_x$ indicating a MIT. The unloaded (presumably $x \sim 2$) film does not show this transition suggestive of a hydrogen concentration greater than $x=2$.

rate with previous YH_x results². The dihydride state was verified by the characteristic transmission peak observed near $\hbar\omega = 1.8$ eV ($\lambda = 700$ nm)^{1,2}. The hydrogen-induced transmittance increase ($\Delta T(\lambda)$) between $x \approx 2$ and fully hydrogenated films at STP for $z \leq 0.10$ is a factor of 3 greater than that of $z = 0.20$, and a factor of 12 greater than that of $z = 1.00$. Additionally, the energy of maximum transmittance for $z > 0.10$ converged to $\hbar\omega = 1.51$ eV ($\lambda = 820$ nm), indicating trihydride formation is no longer observed for these alloys. For films with $z = 0.50$, the fully hydrogenated film transmittance is trihydride-like, with a maximum at the lowest measured energy ($\hbar\omega = 1.29$ eV). This anomalous transmittance due to phase-separated yttrium forming a trihydride was observed for $z = 0.40$ and $z = 0.50$; phase separation was verified by peak splitting in dihydride XRD data. The significance of Sc substitution on the transmittance is further emphasized by considering the spectral density change of fully hydrogenated films relative to dihydride films for each alloy. We define the spectral

density change as

$$\Delta S(x) = \frac{\int T_x d\lambda - \int T_2 d\lambda}{\int T_2 d\lambda},$$

where T_x and T_2 are respectively the transmittance spectra for the fully hydrogenated and dihydride films, and the integration is performed over the full spectral width of the measurements (620 nm). Figure 1(a) shows a significant reduction of the spectral density change with increasing Sc content, implying a quenching of the MIT for $z > 0.10$.

The Lambert-Beer law allows the optical gap to be estimated using the absorption coefficient, $\alpha(\omega)$, in the frequency-dependent transmittance $T(\omega) = T_o \exp[-\alpha(\omega)d]$, where d is the film thickness, and T_o describes the system components that are hydrogen-independent. For parabolic bands¹⁶, $\alpha(\omega) = C(\hbar\omega - E_g)^\nu / (k_B T)$, where C is a fit parameter and ν describes the gap in momentum space¹⁷. Fits only converged for $\nu = 2$ (an allowed, indirect gap). Fig. 1(b) shows the best fit band gap for the alloy system. E_g is approximately 2.8 eV for $z < 0.20$ (in agreement with previous results³), then approaches 2.0 eV with increasing z as the MIT is quenched. The gap enhancement around $z \approx 0.50$ is due to the aforementioned phase separation.

Room temperature resistivity measurements made simultaneously with optical transmittance measurements reveal a z -dependent transition. This is shown in Fig. 1(c), where we plot $\Delta\rho/\rho = (\rho_{atm} - \rho_{x=2})/\rho_{x=2}$. As the scandium content is increased, the magnitude of the MIT decreases until the resistivity remains at the dihydride minimum in Sc films. The resistivity of the rare-earth layer for $z = 0.00$ and $z = 0.10$ when fully hydrogenated is estimated to be 500–1000 $\mu\Omega$ -cm. This greater than an order of magnitude resistivity increase is due to the formation of a trihydride. For $z = 0.20$, the change in resistivity is less than a factor of 2, indicating a suppression in the MIT. Although alloys with $z > 0.10$ show little or no transmittance increase beyond the dihydride concentration (suggesting that the maximum hydrogen concentration is $x \approx 2$), the resistivity increases beyond the dihydride minimum for all alloys with $z \leq 0.90$, which suggests that a fractional amount of hydrogen is able to incorporate beyond $x = 2$ creating random scattering centers.

Surprisingly, the $z=0.1$ films have greater resistivity in the unloaded state rather than in the as-deposited state. Unloaded films are expected to have a dihydride composition that is characterized by a lower resistivity than the parent metals. This, along with the lack of a characteristic transmittance maximum near 700 nm, may suggest the formation of a stable super-dihydride alloy ($x=2+\delta$) for $z=0.1$. Interestingly, the relative hydrogen-induced resistivity change between the as-deposited and trihydride compositions of this alloy is similar to that of $z=0.0$ (Fig1(c) open symbol, \diamond).

The combinatorics can be calculated to determine the fraction of octahedral sites that have a specific num-

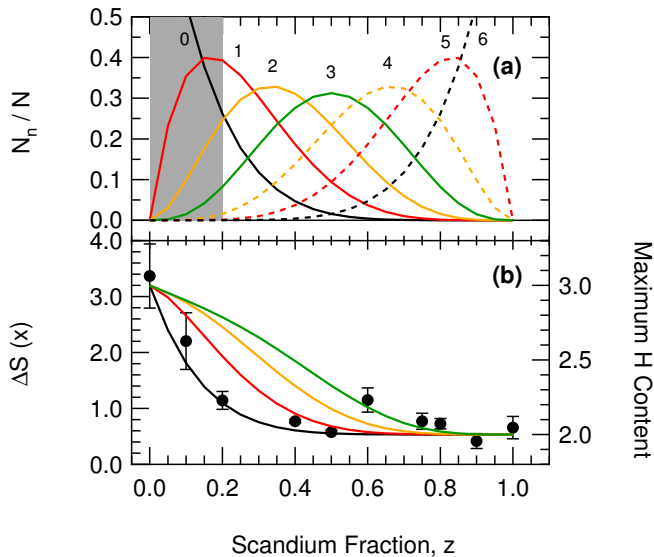


FIG. 2: (Color online) (a) Fraction of octahedral sites that have n Sc nearest neighbors as a function of Sc fraction. Outside of the shaded region the MIT is largely quenched. (b) The change in spectral density transmittance scaled to the H content predicted by restricting octahedral occupancy to sites with (dots experimental) and model curves (from left) $n=0$, $n \leq 1$, $n \leq 2$, and $n \leq 3$ nearest-neighbor Sc.

ber of nearest neighbor Sc atoms. For our samples, we have an fcc lattice with N octahedral sites each having $\xi=6$ nearest-neighbor lattice sites. For a homogeneous $Y_{1-z}Sc_z$ alloy, the fraction of octahedral sites with n Sc nearest neighbor atoms and $\xi - n$ nearest neighbor Y atoms is given by

$$\frac{N_n}{N} = \frac{\xi!}{(\xi-n)!n!} (1-z)^{\xi-n} z^n.$$

Figure 2(a) shows a sharp drop in the fraction of octahedral sites with more than five Y nearest neighbors as the Sc content increases. Assuming it is necessary to have i nearest-neighbor Sc atoms in order to permit octahedral site occupancy, the expected total hydrogen content for each alloy can be calculated as

$$x = 2 + (1-z) \sum_{i=0}^n N_i/N,$$

where N_i/N is the fraction of octahedral sites with i nearest-neighbors. Comparing this relation to the transmittance data reveals that the MIT occurs primarily when octahedral interstices have five or more Y nearest neighbors (Fig. 2(b)). As the Sc content is increased, octahedral sites have fewer Y nearest neighbors, the unit

cell volume accordingly shrinks making it difficult for H to occupy the octahedral sites, and the MIT is thereby quenched.

Studies of pressure-composition isotherms for bulk Y-Sc hydrides support our stoichiometry conclusions¹⁸.

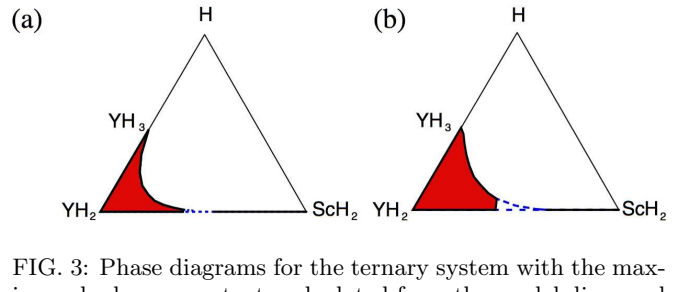


FIG. 3: Phase diagrams for the ternary system with the maximum hydrogen contents calculated from the model discussed in the text. (a) Assumes $n=0$ and (b) $n \leq 1$.

In addition, the immiscibility of YH₂ and ScH₂ has been observed and attributed to differences in atomic radii. Thermodynamically, YH₂ is more stable than ScH₂¹⁸. Hydrogen tend to reside near Y atoms, creating a YH₂/ScH mixture until the dihydride filling is completed. In alloys with near equal proportions of each metal, phase separation is expected due to stresses induced from lattice expansion in YH₂ before forming ScH₂. Phase diagrams generated from this work using the maximum hydrogen concentration calculated as discussed above are shown in Fig. 3. The shaded region represents a solid-solution phase. The dashed lines bound the phase-separation region. Although we have not observed a scandium trihydride in these experiments, high pressure studies may lead to the discovery of this material.

In summary, optical transmittance spectra and electrical resistivity measurements show that the switchable mirror effect in the $Y_{1-z}Sc_zH_x$ alloy system is quenched by the loss of available octahedral sites that results from the reduction of the unit cell volume as Sc concentration is increased. XRD data put this boundary at approximately the same unit cell volume as Lu and corresponds to a previously measured volumetric limit¹⁵. Combinatoric modelling implies a significant loss of octahedral interstices with nearest neighbor Y atoms for Sc fractions greater than 0.10, corroborating the experimentally observed boundary. These observations imply a natural steric boundary for the switchable mirror effect.

Supported by the National Science Foundation Grant No. DMR-0072365 and DMR-0605828, Robert A. Welch Foundation Grant No. F-1191, and the Texas Advanced Technology Program Grant No. No. 003658-0739.

¹ J. N. Huiberts, R. Griessen, J. H. Rector, R. J. Wijngaarden, J. P. Dekker, D. de Groot, and N. J. Koeman, Nature

- ² R. Griessen, J. N. Huiberts, M. Kremers, A. T. M. v. Dekker, and P. H. L. Notten, *J. Alloys Comp.* **253-254**, 44 (1997).
- ³ S. Enache, T. Leeuwerink, A. F. T. Hoekstra, A. Remhof, N. J. Koeman, B. Dam, and R. Griessen, *J. Alloys Comp.* **397**, 9 (2005).
- ⁴ N. L. Adolphi, J. J. Balbach, M. S. Conradi, J. T. Markert, R. M. Cotts, and P. Vajda, *Phys. Rev. B* **53**, 15054 (1996).
- ⁵ E. S. Kooij, J. H. Rector, B. D. D. G. Nagengast, R. Griessen, A. Remhof, and H. Zabel, *Thin Solid Films* **402**, 131 (2002).
- ⁶ A. Remhof, G. Song, D. Laberge, J. Isidorsson, A. Schreyer, F. Güthoff, A. Härtwig, and H. Zabel, *J. Alloys Comp.* **330-332**, 276 (2002).
- ⁷ A. Remhof, J. W. J. Kerssemakers, S. J. van der Molen, R. Griessen, and E. S. Kooij, *Phys. Rev. B* **65**, 54110 (2002).
- ⁸ T. J. Udovic, Q. Huang, R. W. Erwin, B. Hjörvarsson, and R. C. C. Ward, *Phys. Rev. B* **61**, 12701 (2001).
- ⁹ T. J. Udovic, Q. Huang, and J. J. Rush, *Phys. Rev. B* **61**, 6611 (2000).
- ¹⁰ A. T. M. van Gogh, D. G. Nagengast, E. S. Kooij, N. J. Koeman, J. H. Rector, R. Griessen, C. F. J. Flipse, and R. J. J. G. A. M. Smeets, *Phys. Rev. B* **63**, 195105 (2001).
- ¹¹ A. T. M. van Gogh and R. Griessen, *J. Alloys Comp.* **330-332**, 338 (2002).
- ¹² D. G. Nagengast, A. T. M. van Gogh, E. S. Kooij, B. Dam, and R. Griessen, *Appl. Phys. Lett.* **75**, 2050 (1999).
- ¹³ J. Isidorsson, I. A. M. E. Giebels, E. S. Kooij, N. J. Koeman, J. H. Rector, A. T. M. van Gogh, and R. Griessen, *Electrochimica Acta* **46**, 2179 (2001).
- ¹⁴ T. C. Messina, C. W. Miller, and J. T. Markert, *J. Alloys Comp.* **356-357**, 181 (2003).
- ¹⁵ G. Westlake, *J. Less-Common Metals* **74**, 177 (1980).
- ¹⁶ E. J. Johnson, *Semiconductors and Semimetals* (Academic Press, 1967).
- ¹⁷ R. Ahuja, B. Johansson, J. M. Wills, and O. Eriksson, *Appl. Phys. Lett.* **71**, 3498 (1997).
- ¹⁸ M. L. Lieberman and P. G. Wahlbeck, *J. Phys. Chem.* **69**, 3973 (1965).